Journal of Alloys and Compounds 615 (2014) S401–S405

Contents lists available at ScienceDirect

Journal of Alloys and Compounds

journal homepage: www.elsevier.com/locate/jalcom

Microstructure and mechanical properties of 6061 Al alloy based composites with SiC nanoparticles

A.J. Knowles [a], X. Jiang [a], M. Galano [a,*], F. Audebert [a,b,c]

[a] Department of Materials, University of Oxford, Parks Road, Oxford OX1 3PH, Oxfordshire, UK
[b] Advanced Materials Group, Faculty of Engineering, University of Buenos Aires, Buenos Aires, Paseo Colón 850, Ciudad de Buenos Aires 1063, Argentina
[c] Department of Mechanical Engineering and Mathematical Sciences, Oxford Brookes University, Wheatley Campus, Oxford OX33 1HX, UK

ARTICLE INFO

Article history:
Available online 27 January 2014

Keywords:
Al alloys
Powder metallurgy
Metal matrix composites
Mechanical properties

ABSTRACT

Materials with high specific strengths as well as damage tolerance are of great importance for automotive and aerospace applications. Ceramic reinforced metal matrix composites (MMCs) show good potential for these uses but have been hampered by insufficient ductility and production issues, both of which this work looks to resolve. Nanoparticle reinforced 6061 aluminium alloy matrix composites have been produced by a powder metallurgy route and shown to exhibit high strength and Young's modulus alongside good ductility and low density.

A powder metallurgy route consisting of high energy ball milling, hot isostatic pressing (HIP) and extrusion has proved a highly effective process for achieving a homogeneous distribution of particles, with minimal clustering of the nanoparticles, at an industrially relevant scale. After heat treatment the composites display high strengths, owing to SiC nanoparticle reinforcement as well as the age hardening effect. The remarkable feature of nanoparticle reinforced MMCs compared to micron size reinforcements is that particle fracture does not occur and effective particle–matrix bonding can be taking place, resulting in a greater combination of strength and toughness.

The combination of properties achieved by the composites studied in this work are superior to most of the micron sized particle reinforced MMCs reported elsewhere and are well beyond what is possible with traditional aluminium alloys.

1. Introduction

Particle reinforced metal matrix composites (MMCs) are attractive materials for automotive and aeronautic applications due to their high strengths and low densities. They are also interesting for their high temperature behavior, good creep and wear resistance, higher stiffness than Al alloys and ageing response [1–3].

Particle containing MMCs have significant benefits in processability over continuous fiber MMCs but tend to have lower ductility. The majority of studies have concentrated on the mechanical properties of Al alloy composites reinforced with micro-sized particles [4,5]. The effects of nano-sized reinforcements on the mechanical properties have not been thoroughly studied [6]. This class of MMCs has been shown to realise high strengths alongside respectable ductility, but are reliant on homogeneous microstructures [7] and are more complicated to process, typically using powder metallurgy (PM) techniques [8].

Aluminium alloys are regularly chosen as a matrix because of their low density, good isotropic mechanical properties, excellent corrosion resistance and reasonable cost. Amongst aluminium alloys, 6061 is an Al–Mg–Si alloy widely used for structural applications due to its good strength, weldability, corrosion resistance, immunity to stress corrosion cracking as well as heat treatability, forming precipitates that increase the strength at the cost of somewhat reduced ductility [9,10]. SiC is commonly chosen as a reinforcement phase due to its suitable properties, such as high strength, Young's modulus, thermal shock resistance, and because it can form a strong bond to aluminium [11]. The matrix–particle interface strength is important as it governs the efficiency of load transfer, affecting the strengthening, as well as the ease of decohesion, which has implications for the composite's failure mechanism [12]. The formation of Al_4C_3 in Al/SiC composites degrades the particles and the fibers, and results in composites with poor mechanical properties. Therefore, during the composite fabrication, three primary techniques have been employed for controlling the deleterious interfacial reactions: (1) modification of matrix chemical composition: for example, Si was added into the aluminum alloy

* Corresponding author.
E-mail address: marina.galano@materials.ox.ac.uk (M. Galano).

http://dx.doi.org/10.1016/j.jallcom.2014.01.134
0925-8388/

matrix, in order to hinder the above interfacial reaction [13]; (2) surface reinforcement modification: the surface reinforcement modification by coating or passive oxidation has been successful to some extent in preventing the detrimental interfacial reaction and enhancing the materials wettability [14,15]; (3) processing parameter is controlled so that the extent of the interfacial reaction can be limited. Examples are controlling the processing temperature and holding time during composite fabrication. Thereby, the various composite processing methods such as compocasting, squeeze casting, semisolid forming, spray forming, and powder metallurgy can be used for the composite fabrication [8,16,17].

The two main parameters related to the reinforcement particles are the volume fraction and size of the reinforcing particles. With increasing particles' volume fraction the strength is improved due to a greater number of dislocation barriers but at the cost of reduced ductility, as deformation is localised on a smaller volume of the plastic matrix which is then less able to accommodate the deformation [18]. An increase in strength can be obtained with decreasing particle size, owing to a greater number of particles for the same volume fraction, whilst at the same time ductility is preserved because, below a critical size, particles no longer fracture [4]. As well as Orowan strengthening, particles pin grain boundaries, stabilise substructure cells, can accelerate the ageing response and increase the work hardening rate [10,19]. Particularly, an accelerated ageing process was observed in Al alloy matrix composites reinforced with SiC particles due to the thermal expansion coefficient (CTE) differences between the Al matrix and the SiC reinforcement [20].The present work aims to develop high-strength, ductile and low density composites for structural applications. It focuses on novel Al 6061 alloy composites reinforced with SiC produced by means of a powder metallurgy process using SiC nanoparticles (<500 nm) and a low temperature ageing treatment.

2. Experimental procedure

Composite billets with 10 wt% and 15 wt% SiC reinforcement particles with average size lower than 500 nm diameter were provided by Aerospace Metal Composites Ltd. (AMC). These were produced by a proprietary process including high energy ball milling followed by hot isostatic pressing (HIP).

To allow comparisons to be made, an unreinforced alloy was produced from sieved Al 6061 powder, average diameter 10 μm. This was cold unidirectionally compacted with a load of 50 Tons to produce billets of 30 mm diameter and 30 mm height.

All these materials were then extruded in a Fogg & Young extruder with an extrusion ratio of 14:1 obtaining bars of 7.5 mm in diameter and ~1 m in length. Samples were heated to 450 °C in 15 min and held for 20 min prior to extrusion. An extrusion speed of 8 mm/s was used. After extrusion the samples were allowed to air cool.

Following extrusion, a solutionising, T4, heat treatment at 525 °C for 1 h was applied followed by water quenching. An artificial ageing, T6, treatment was then performed at 125 °C for 8 h followed by air cooling. A lower ageing temperature was used in contrast with that normally used in the literature (160 to 185 °C) in order to obtain a very refined precipitation and higher ductility and toughness. It is expected that at this low temperature it can be obtained an optimum T6 condition for the composites and strong bonds between the SiC and the Al matrix without brittle particles formed at the Al–SiC interface [10,19–21].

Microstructural characterisation was performed in the pre-extruded, as-extruded, solutionised and aged states. For this X-ray diffractometry (XRD) was carried out in a $\theta-2\theta$ diffractometer Philips 1810 using Cu Kα radiation, voltage of 35 kV, current of 50 mA and step size 0.02°, while scanning electron microscopy (SEM) was performed on JEOL 6300 and JEOL 840A with an energy dispersive X-ray spectrometer (EDX), and JEOL 840F field emission gun (FEG) microscope. Transmission election microscopy (TEM) was performed on a Philips CM20 and a JEOL 2000FX with an energy dispersive X-ray spectrometer (EDX).

After microstructural characterisation the mechanical properties were evaluated. Microhardness measurements were performed on a Wilson Instruments Vickers microhardness tester with a load of 500 g for 20 s. The values recorded for each sample were made from an average of 20 indents across the extruded bar. In addition, tensile tests were performed on a 100 kN Instron tensile test machine, at room temperature at a strain rate of 10^{-4} s^{-1}. The samples were machined to ASTM standard 'E 8 small-size specimen 4' with 16.0 ± 0.1 mm gage length, 4.0 ± 0.1 mm gage diameter. Two specimens of each material were tested to evaluate the consistency of the response.

3. Results and discussion

3.1. Microstructural characterisation

Fig. 1 shows the X-ray diffractograms of cross sections of the samples in the as-extruded and aged conditions. The α-Al peaks are clearly visible. The peak observed for the 6061 alloy and composites at ~36.5° remained after the ageing heat treatment and was assigned to the α-AlFeSi intermetallic [22]. Lastly, peaks of the 6H–SiC phase can be seen in the two composites; with higher peak intensities for the 15 wt% SiC sample, as would be expected. No peaks of the Al_4C_3 phase were observed, suggesting that little or no interfacial reaction has occurred, which is known to embrittle the composite when present [11].

The higher relative intensity of the peak (1 1 1) with respect to the standard pattern for the Al suggests Al grain texture in {1 1 1} along the extrusion direction, as has been seen by Poudens et al. [23].

Secondary electron images of the composites in the as-extruded condition are shown in Fig. 2 in which a homogenous distribution of blocky <500 nm particles, identified as SiC by EDX, are seen. No clustered particles were observed. Samples were also analysed in the heat treated state, with no major difference in the microstructure observed.

TEM bright field images representative of the as-extruded 6061 Al alloy and composite samples are shown in Fig. 3. It can be seen that the 6061 Al alloy in the as-extruded condition has <100 nm precipitates within the Al grains and also at the grain boundaries, as shown by the arrows (Fig. 3(a)). A combination of <500 nm SiC particles and the <100 nm precipitates can be seen for the SiC composites in the as-extruded condition (Fig. 3(b) and (c)). EDX was carried out on particle A (Fig. 3(d)) and particle B (Fig. 3(e)) in the as-extruded composites and the result is displayed in Fig. 3(f), strongly suggesting that these particles are SiC. During TEM analysis no clear aluminium carbides or intermetallics were observed at the Al matrix–SiC particle interface, agreeing with the XRD findings. As the SiC in Al is thermodynamically unstable the Al_4C_3 phase is normally formed at the interface during the composite fabrication with the melted Al or with the solid state Al matrix during long time at high temperature treatments [16,20,24]. Other authors also observed intermetallic precipitates at the Al matrix–SiC interface, for example, Mahon et al. [20] observed fine intermetallics containing Mg and Cu precipitated at the Al 2124 matrix–SiC interface after an ageing treatment at

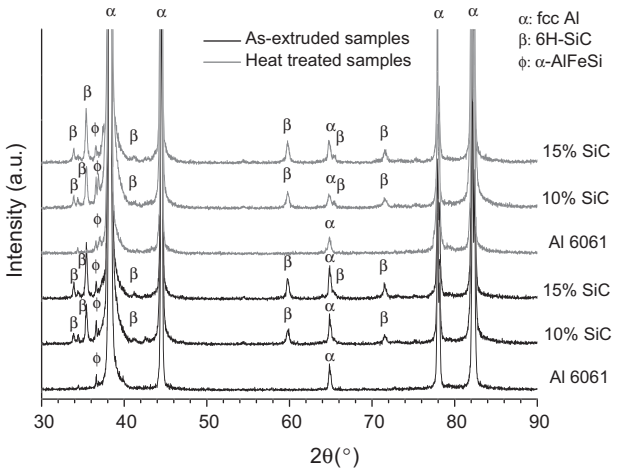

Fig. 1. X-ray diffractograms of cross sections of the samples in the as-extruded and heat treated conditions.

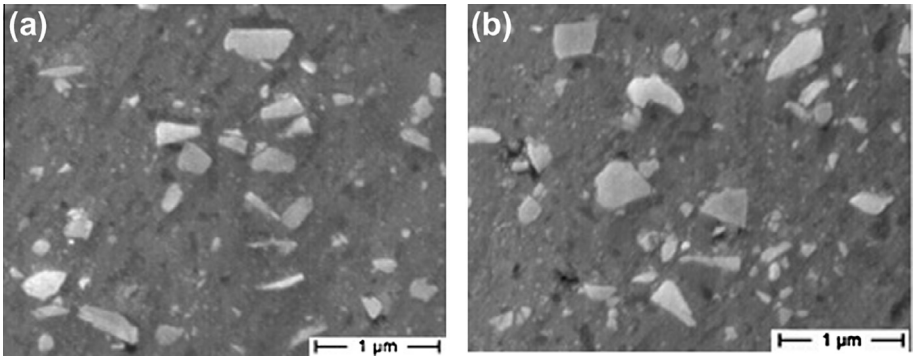

Fig. 2. Secondary electron images of (a) 10 wt% SiC composite and (b) 15 wt% SiC composite in the as-extruded condition.

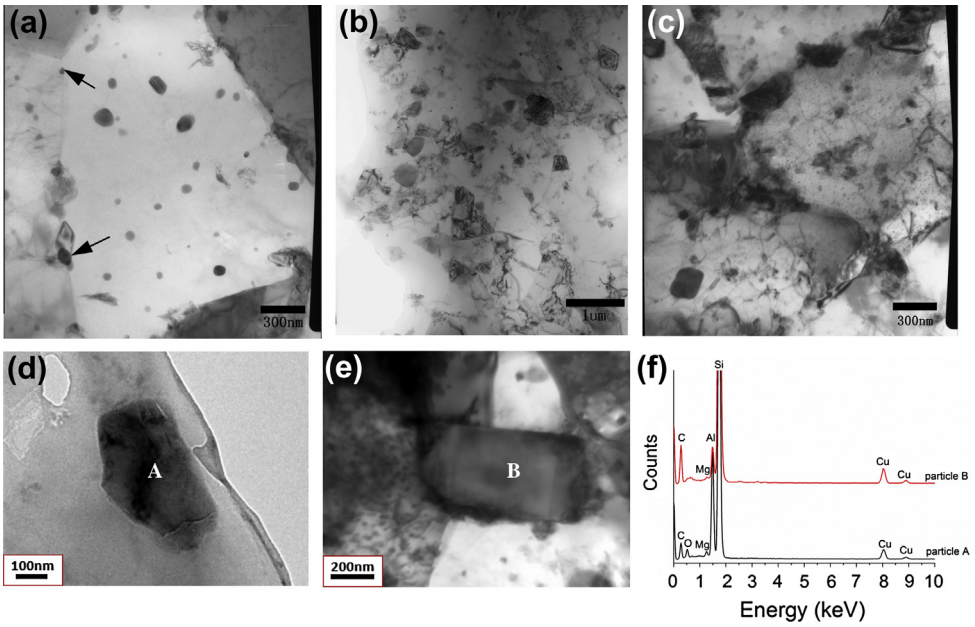

Fig. 3. TEM Bright field images of (a) as-extruded 6061 Al alloy (arrows show precipitates at a grain boundary), (b) as-extruded 10 wt% SiC, (c) as-extruded 15 wt% SiC samples, (d) a SiC particle 'A' in 10 wt% SiC, (e) a SiC particle 'B' in 15 wt% SiC and (f) EDX results on particle 'A' and 'B'.

177 °C for 8 h. In the present work the whole process was performed in the solid state and the ageing treatment was carried out for 8 h at 125 °C which hindered the formation of any carbide and intermetallics at the Al matrix–SiC particle interface. The microstructure of the composites has been found to have an even dispersion of blocky <500 nm SiC particles within the 6061 alloy matrix that also contains smaller, <100 nm, intermetallic precipitated inside the Al grains and at the Al grain boundaries, produced during the extrusion and the thermal treatment of the composites.

3.2. Mechanical properties

The results of microhardness testing are summarised in Table 1. A clear trend of increasing hardness with volume fraction of reinforcement is seen in both the as-extruded and aged conditions. Also notable is that the SiC containing composites exhibit a greater increase in hardness after heat treatment, which is thought to be due to the SiC particles facilitating an improvement in ageing response, as it was observed previously for other Al based composites [25,26]. This has been attributed partially to the presence of a high dislocation density around particles, generated during cooling due to the thermal expansion coefficient (CTE) differences. The dislocations are punched out at the reinforcement–matrix interfaces to relax the stress generated due to the mismatch in the CTEs of Al ($24 \times 10^{-6}\,K^{-1}$) and SiC ($4 \times 10^{-6}\,K^{-1}$) [27,28]. The greater dislocation density would increase solute atom diffusion rates as well as reducing the activation energy for nuclei formation [25,26,29,30]. Due to this effect the composites may reach their peak hardness after shorter heat treatment times or at lower temperature than the unreinforced alloy [26].

The tensile engineering stress–strain curves are shown in Fig. 4, and the material properties evaluated from them, in Table 1. There is a clear trend of increasing yield stress (0.2% offset), ultimate tensile stress (UTS) and Young's modulus with increasing particle volume fraction. The increase in Young's modulus (E) implies there is good load transfer occurring between the particles and matrix, by a strong bonding between Al and SiC [11,33]. The values achieved are high for particle based composites, which are inherently limited in the extent of loading possible as is the case for short fiber composites [34]. The E values measured for the 6061 Al alloys and SiC_p composites studied are in correlation with the E values reported for the commercial composites summarized in Table 1.

The yield stress and the UTS values obtained are also in correlation with the corresponding values reported for the commercial composites summarized in Table 1.

The strain to failure decreases with SiC_p volume fraction, as would be expected when adding a brittle component. However, the decrease is not as severe as is often seen with micron sized

Table 1
Summary of mechanical properties of the 6061 Al alloy and their SiC_p composites studied and for comparison commercially produced composites with micron sized reinforcements from Alcan [31] and DWA composites [32] are also shown. Vickers microhardness in as-extruded and aged conditions, tensile testing results: Young's modulus (E), yield stress (σ_y, 0.2% offset), ultimate tensile strength (UTS), strain to failure (ε_f), energy to fracture (calculated by the area under the stress strain curves) and average dimple size, in as-extruded and aged conditions.

Material	Vickers microhardness (μHV_{500} ± S.D.)	Average values of tensile tests As-extruded samples (E) Heat treated samples (HT)					
	As-extruded heat treated (E) Heat treated (HT)	E (GPa)	σ_y (MPa)	UTS (MPa)	ε_f (%)	Energy to fracture ($J\,m^{-3}$)	Avg. dimple size (μm)
Al 6061 (E)	57.4 ± 1.1	68.5	131	205	16.5	30	1.22
Al 6061 (HT)	82.1 ± 1.8	69.5	226	342	20.5	55.5	1.11
Al 6061 + 10 wt% SiC (E)	88.1 ± 1.8	87	192	287	15	39.5	1.42
Al 6061 + 10 wt% SiC (HT)	126.1 ± 2.0	90	281	424	17	58.5	0.93
Al 6061 + 15 wt% SiC (E)	101.9 ± 2.0	103	229	329	14	41	1.45
Al 6061 + 15 wt% SiC (HT)	137.6 ± 1.7	99	307	449	15.5	56	0.98
Al 6061 T6 + 15 vol% SiC * Cospray Alcan [31]	–	96	350	420	8	–	–
Al 6092 T6 + 17.5 vol% SiC * DWA [32]	–	105.5	400	460	3	–	–

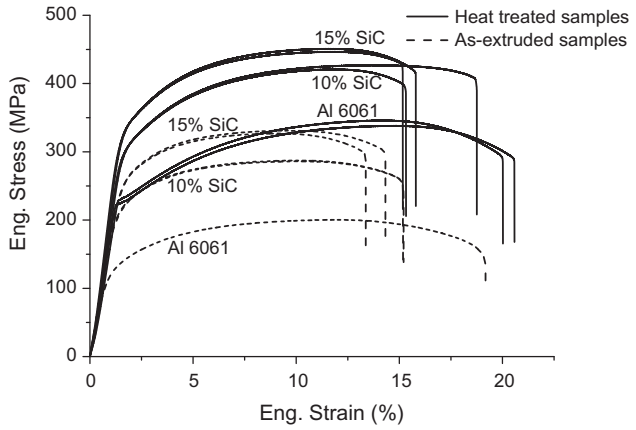

Fig. 4. Engineering stress–strain curves of 6061 Al alloy and 10 wt% SiC and 15 wt% SiC composites samples in the as-extruded and heat treated conditions.

reinforcements, such as those shown in Table 1 for commercial composites produced by co-spray by Alcan International Ltd. [31] and DWA Aluminum Composites [32]. It is worth noting that the strain to failure obtained for 15 wt% SiC_p (<500 nm) composite is 2 times higher than that developed by co-spray by Alcan for the same matrix and volume fraction of SiC particles but with μm size [31]. It should be noted that because of the increase in strength and the small reduction in strain the area under the stress–strain tensile curves (energy to fracture), which is an indication of "static toughness", is maintained for the composites studied.

The maintenance of the energy to fracture with reinforcing particles present can be in part attributed to the particles being sufficiently small that there is no chance of a fracture event occurring within the particle. This is due to (i) good particle distribution with no clustering since clusters are known to fail prematurely and are less effective at transferring loads [35] and (ii) the reduced stress within each particle as well as the reduction in flaw size [5]. The trends observed can be seen in both the as-extruded and heat treated conditions with a large boost in properties achieved by the heat treatment. The low temperature ageing treatment chosen (125 °C for 8 h) improved all the mechanical properties values, microhardness, yield stress, UTS, Young's modulus and even the strain to failure. As a main consequence the "energy to failure" has been increased strongly. This benefit can be explained by a strong bond between Al matrix and SiC particles with no brittle phase precipitating at the interface, and very fine precipitates distribution inside the Al grains.

The fractured surfaces of the samples tested are shown in Fig. 5. All the samples showed failure by macro-void coalescence due to the ductile 6061 alloy matrix. This would be expected because particles often initiate voids, as has been observed in micron reinforced composites [36] but the average void size (see Table 1) was found to have little change with the addition of the nanoparticles. It was not clear whether voids systematically contained ceramic particles as few were found with particles, but the empty voids may have lost their initiating particle after fracture. There

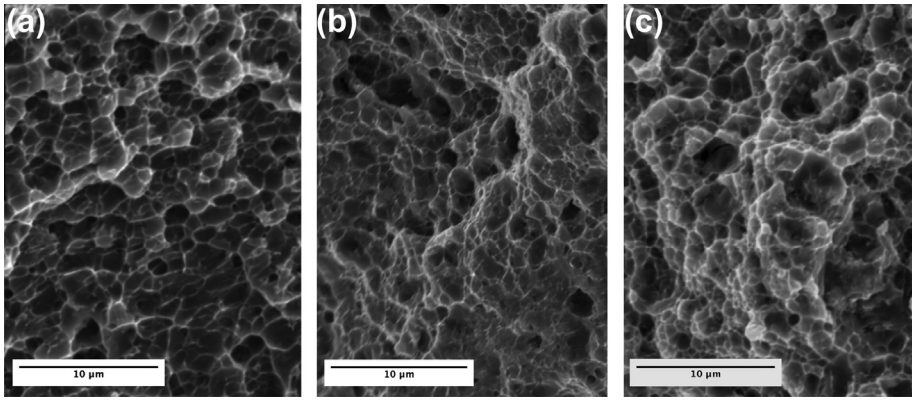

Fig. 5. Fractography of (a) 6061 alloy, (b) 10 wt% SiC and (c) 15 wt% SiC all in the as-extruded condition.

was also no evidence of single particle fracture. The lack of particle fracture can be attested by the fact that no drop in the Young's modulus was observed after small strains. Such a drop is typical for composites with larger sized particles, where particle fracture occurs during the early stages of straining, reducing their stiffening effect [20].

The smaller dimple size found for the aged samples respect to the as-extruded samples could be related to the very fine distribution precipitates obtained by the low heat treatment temperature.

4. Conclusions

The powder metallurgy route used, consisting of high energy ball milling, HIP and then extrusion, was found to be an effective method of producing composites with a homogeneous distribution of particles, without clustering which led to maximise the benefits that particle reinforcement brings to the mechanical properties.

The process and the heat treatment used for the artificial ageing during 8 h at 125 °C allowed hindering the formation of the detrimental Al_4C_3 and brittle intermetallics at the Al matrix–SiC particle interface, but obtaining a strong particle–matrix bonding which allows an effective load transfer that results in an effective improvement in the Young's modulus.

The fine SiC reinforcement sizes (<500 nm) used contribute to more efficient strengthening of the composites than a similar volume fraction of larger particles, because there are a greater number of barriers to dislocations and the particles do not fracture during the deformation, which results in high strength preserving the "energy to fracture" under tensile stress deformation.

The composites produced in this research, combining the use of small SiC particles (<500 nm) and low ageing temperature, display high strength and hardness whilst maintaining remarkable ductility. The combination of these properties is superior to existing alloys and similar composites.

Acknowledgements

The authors thank AMC for the supply of starting composite billets, ALPOCO for the aluminium powder, as well as Dr. I. Dyson for access to the tensile testing rig. M. Galano thanks the RAEng for the support in her research. F. Audebert and M. Galano give thanks for PICT-Oxford 2831 grant.

References

[1] K.U. Kainer, Kovine Zlitine Technologije 30 (6) (1996) 509–516.
[2] A. Kelly, Compos. Sci. Technol. 23 (1985) 171–199.
[3] A. Manna, B. Bhattacharyya, Inst. Eng. (India) J. Prod. 83 (2003) 46–50.
[4] V.V.B. Prasad, B.V.R. Bhat, Y.R. Mahajan, P. Ramakrishnan, Mater. Sci. Eng. A 337 (2002) 179–186.
[5] Z.W. Wang, M. Song, C. Sun, D.H. Xiao, Y.H. He, Mater. Sci. Eng. A 527 (2010) 6537–6542.
[6] N. Chawla, Y.L. Shen, Adv. Eng. Mater. 3 (2001) 357–370.
[7] Y.C. Kang, S.L.I. Chan, Mater. Chem. Phys. 85 (2004) 438–443.
[8] C. Suryanarayana, J. Alloys Comp. 509 (2011) S229–S234.
[9] R.E. Sanders, Min. Met. Mater. Sci. 53 (2001) 21–25.
[10] I.J. Polmear, Light Alloys: Metallurgy of the Light Metals, third ed., Arnold, London, 1995.
[11] J.A. Ballantine, J.J. Conner, J.L. Handrock, Fundamentals of Metal Fatigue Analysis, first ed., Prentice Hall, 1990.
[12] T.W. Clyne, P.J. Withers, An Introduction to Metal Matrix Composites, First paperback ed., Cambridge University Press, Cambridge, 1993. 1995.
[13] J.-Ch. Lee, J.-Y. Byun, S.-B. Park, H.-I. Lee, Acta Mater. 46 (5) (1998) 1771.
[14] M. Gu, Z. Mei, Y. Jin, Z. Wu, Scr. Mater. 40 (9) (1999) 985.
[15] Z. Shi, J.M. Yang, J.C. Lee, D. Zhang, H.I. Lee, R. Wu, Mater. Sci. Eng. A 303 (2001) 46–53.
[16] O. Beffort, S. Long, C. Cayron, J. Kuebler, Ph.-A. Buffat, Compos. Sci. Technol. 67 (2007) 737–745.
[17] K. Mizuuchi, K. Inoue, Y. Agari, T. Nagaoka, M. Sugioka, M. Tanaka, T. Takeuchi, J.-I. Tani, M. Kawahara, Y. Makino, M. Ito, Compos.: Part B 43 (2012) 2012–2019.
[18] S.J. Hong, H.M. Kim, D. Huh, C. Suryanarayana, B.S. Chun, Mater. Sci. Eng. A 347 (2003) 198–204.
[19] H.S. Chu, K.S. Liu, J.W. Yeh, Metall. Mater. Trans. A 31 (2000) 2587–2596.
[20] G.J. Mahon, J.M. Howe, A.K. Vasudevan, Acta Metall. Mater. 38 (1990) 1503–1512.
[21] F. Hayat, Mater. Sci. Eng. A 556 (2012) 834–843.
[22] A. Verma, S. Kumar, P.S. Grant, K.A.Q. O'Reilly, J. Alloys Comp. 555 (2013) 274–282.
[23] A. Poudens, B. Bacroix, T. Bretheau, Mater. Sci. Eng. A 196 (1995) 219–228.
[24] B. Xiong, Z. Xu, Q. Yan, B. Lu, Ch. Cai, J. Alloys Comp. 509 (2011) 1187–1191.
[25] N. Parvin, R. Assadifard, P. Safarzadeh, S. Sheibani, R. Marashi, Mater. Sci. Eng. A 492 (2008) 134–140.
[26] H.K. Ahn, C.H. Yu, Met. Mater. Korea 7 (2001) 1–7.
[27] K.K. Chawla, M. Metzer, J. Mater. Sci. 7 (1972) 34–39.
[28] R.J. Arsenault, N. Shi, Mater. Sci. Eng. A 81 (1986) 175–187.
[29] H.R. Shakeri, Z.R. Wang, Metall. Mater. Trans. A 33 (2002) 1699–1713.
[30] P. Rodrigo, P. Poza, M.V. Utrilla, A. Urena, J. Alloys Comp. 482 (2009) 187–195.
[31] A. Miravete, Metal matrix composites: Proceedings of the Ninth International Conference on Composite Materials (ICCM/9) Madrid, 12–16 July, 1993, University of Zaragoza, Woodhead Publishing, Zaragoza, Cambridge, 1993.
[32] http://www.dwa-dra.com/downloads/6092Props082012.pdf (20.12.2013).
[33] W.D. Fei, X.D. Jiang, C. Li, C.K. Yao, J. Mater. Sci. Lett. 15 (1996) 1966–1968.
[34] H. Fukuda, K. Kawata, Fibre Sci. Technol. 7 (1974) 207–222.
[35] Z.Y. Liu, Q.Z. Wang, B.L. Xiao, Z.Y. Ma, Compos. Part A: Appl. Sci. Manuf. 41 (2010) 1686–1692.
[36] T.S. Srivatsan, M. Al-Hajri, C. Smith, M. Petraroli, Mater. Sci. Eng. A 346 (2003) (2009) 91–100.